Engineering Science and Technology, an International Journal xxx (2015) 1–8

HOSTED BY

Contents lists available at ScienceDirect

Engineering Science and Technology, an International Journal

journal homepage: http://www.elsevier.com/locate/jestch

Full length article

Power sharing algorithm for vector controlled six-phase AC motor with four customary three-phase voltage source inverter drive

Sanjeevikumar Padmanaban [a,*], Gabriele Grandi [a], Frede Blaabjerg [b], Joseph Olorunfemi Ojo [c], Patrick William Wheeler [d]

[a] Department of Electrical, Electronic, and Information Engineering, Alma Mater Studiorum 1088AD, University of Bologna, 40136 Bologna, Italy
[b] Department of Energy Technology, Aalborg University, Pontoppidanstraede 101, 9220 Aalborg, Denmark
[c] Center for Energy System Research, Department of Electrical & Computer Engineering, Tennessee Technological University, 38505 Cookeville, TN, USA
[d] Power Electronics, Machines and Control Group, Department of Electrical & Electronics Engineering, Nottingham University, NG7 2RD Nottingham, UK

ARTICLE INFO

Article history:
Received 14 October 2014
Received in revised form
19 January 2015
Accepted 11 February 2015
Available online xxx

Keywords:
Open-end winding machines
Multi-phase machines
Power sharing algorithm
Field oriented control
Multi-phase space vectors
Multi-phase inverter
Classical voltage source inverter

ABSTRACT

This paper considered a six-phase (asymmetrical) induction motor, kept 30° phase displacement between two set of three-phase open-end stator windings configuration. The drive system consists of four classical three-phase voltage inverters (VSIs) and all four dc sources are deliberately kept isolated. Therefore, zero-sequence/homopolar current components cannot flow. The original and effective power sharing algorithm is proposed in this paper with three variables (degree of freedom) based on synchronous field oriented control (FOC). A standard three-level space vector pulse width modulation (SVPWM) by nearest three vectors (NTVs) approach is adopted to regulate each couple of VSIs. The proposed power sharing algorithm is verified by complete numerical simulation modeling (Matlab/Simulink-PLECS software) of whole ac drive system by observing the dynamic behaviors in different designed condition. Set of results are provided in this paper, which confirms a good agreement with theoretical development.

1. Introduction

For the past 30 years the technology of multi-phase machines had proved that they are predominant solution over their classical three-phase ac machines counterpart [1–3]. In specific by increased reliability, redundant structure, reduced torque ripple, increased torque density, fault tolerability, and reduced per-phase of inverter rating [2]. Furthermore, for any m-phase machines ($m > 3$) only two currents are sufficient to control the torque/flux independently, even if with reduced performance [2]. Multi-phase configurations, in particular six-phase machines, are the foremost choice for high power (low voltage/high current) applications, where two adjacent windings are spatially shifted by 60° (symmetrical type) [3] or by 30° (asymmetrical or dual three-phase type) [4–11].

Literatures are focused on modeling/controlling of six-phase (asymmetrical/symmetrical) machines with indirect/direct, synchronous/stationary field oriented control (FOC), direct torque control (DTC) [6–9], pulse width modulations (PWMs) techniques [12–19], parallel/series operation of multi-phase machines with single inverter drive [1,2,4], and fault tolerant strategies [19–27]. But kept starving for proper and effective power sharing algorithm for six-phase ac machine driven by multi-phase ac drive (VSIs).

This paper investigates a six-phase (asymmetrical or dual three-phase) induction motor with open-end stator windings configuration, as shown by Fig. 1. Priorities in selecting such machines over symmetrical version are described in Refs. [5,10–12]. The drive circuit consists of four classical three-phase voltage source inverters (VSIs) and each inverter is connected across the open-end of two three-phase stator windings. The resultant configuration is a multi-phase inverter motor drive, as shown in Fig. 2. To be noted, all the four dc sources are completely isolated and the entire circuit is absolutely free of zero-sequence/homopolar components.

Further, an original power sharing algorithm based on synchronous field oriented control (FOC) was proposed in this paper with three variables (three degree of freedom) [25,26]. First

* Corresponding author.
E-mail addresses: sanjeevipowerelectronics@gmail.com, sanjeevi_12@yahoo.co.in (S. Padmanaban).
Peer review under responsibility of Karabuk University.

http://dx.doi.org/10.1016/j.jestch.2015.02.002

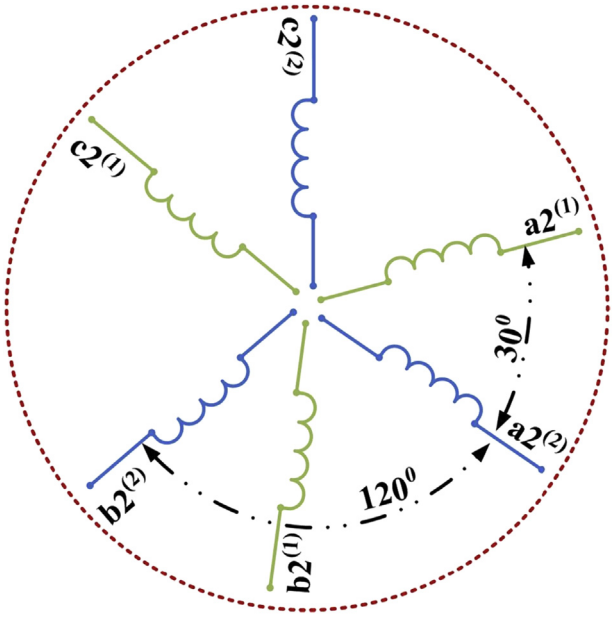

Fig. 1. Six-phase asymmetrical (quasi) induction motor open-end stator windings.

variable provides the proper currents sharing between two three-phase open-end stator windings. Other two provides the proper voltages sharing between each two inverters of two three-phase open-end stator windings. Investigation are focused in particular to dynamic behaviors of the six-phase induction motor direct–quadrature (d–q) axis components, subjected to balanced/unbalanced conditions to verify the effectiveness of the theoretical developments.

2. Six-phase orthogonal space vector transformation

Six-phase orthogonal space vector transformation in sinusoidal rotating frame is given by [12,16–18,28,29]:

$$\bar{x}_h = \frac{1}{3}\left[x_1 + x_2\alpha^h + x_3\alpha^{4h} + x_4\alpha^{5h} + x_5\alpha^{8h} + x_6\alpha^{9h}\right], \quad (1)$$

where $h = 1, 3, 5$ and $X_1 \ldots X_6$ are variables of voltage or current and $\alpha = \exp(j\pi/6)$. Now substituting index h in Eq. (1), leads to:

$$\begin{cases} \bar{x}_1 = \frac{1}{3}\left[x_1 + x_2\alpha + x_3\alpha^4 + x_4\alpha^5 + x_5\alpha^8 + x_6\alpha^9\right] \\ \bar{x}_3 = \frac{1}{3}\left[(x_1 + x_3 + x_5) + j(x_2 + x_4 + x_6)\right] \\ \bar{x}_5 = \frac{1}{3}\left[x_1 + x_2\alpha^5 + x_3\alpha^8 + x_4\alpha + x_5\alpha^4 + x_6\alpha^9\right]. \end{cases} \quad (2)$$

Inverse of Eq. (2) is written as:

$$\begin{cases} x_1 = \bar{x}_3 \cdot 1 + \left(\bar{x}_1 + \bar{x}_5^*\right)\cdot 1 \\ x_3 = \bar{x}_3 \cdot 1 + \left(\bar{x}_1 + \bar{x}_5^*\right)\cdot \alpha^4 \\ x_5 = \bar{x}_3 \cdot 1 + \left(\bar{x}_1 + \bar{x}_5^*\right)\cdot \alpha^8 \end{cases}, \quad \begin{cases} x_2 = \bar{x}_3 \cdot j + \left(\bar{x}_1 - \bar{x}_5^*\right)\cdot \alpha \\ x_4 = \bar{x}_3 \cdot j + \left(\bar{x}_1 - \bar{x}_5^*\right)\cdot \alpha^5 \\ x_6 = \bar{x}_3 \cdot j + \left(\bar{x}_1 - \bar{x}_5^*\right)\cdot \alpha^9, \end{cases} \quad (3)$$

where "*" and "·" denote complex conjugate and scalar product, respectively. The space vectors $\bar{x}_1$, $\bar{x}_3$, $\bar{x}_5$ lie in the planes d_1–q_1, d_3–q_3, d_5–q_5 respectively.

2.1. Equivalent two three-phase space vector transformation

For the purpose of simplification in analysis, space vector transformations given by Eqs. (2) and (3) are split and given as below:

$$\begin{cases} x_1^{(1)} = x_1 \\ x_2^{(1)} = x_3 \\ x_3^{(1)} = x_5 \end{cases}, \quad \begin{cases} x_1^{(2)} = x_2 \\ x_2^{(2)} = x_4 \\ x_3^{(2)} = x_6. \end{cases} \quad (4)$$

The two three-phase space vectors $\bar{x}^{(1)}$, $\bar{x}^{(2)}$ and zero-sequence components $x_0^{(1)}$, $x_0^{(2)}$ of six-phase machine would be written as:

$$\begin{cases} \bar{x}^{(1)} = \frac{2}{3}\left[x_1^{(1)} + x_2^{(1)}\alpha^4 + x_3^{(1)}\alpha^8\right] \\ x_0^{(1)} = \frac{1}{3}\left[x_1^{(1)} + x_2^{(1)} + x_3^{(1)}\right] \end{cases}, \quad \begin{cases} \bar{x}^{(2)} = \frac{2}{3}\left[x_1^{(2)} + x_2^{(2)}\alpha^4 + x_3^{(2)}\alpha^8\right] \\ x_0^{(2)} = \frac{1}{3}\left[x_1^{(2)} + x_2^{(2)} + x_3^{(2)}\right]. \end{cases} \quad (5)$$

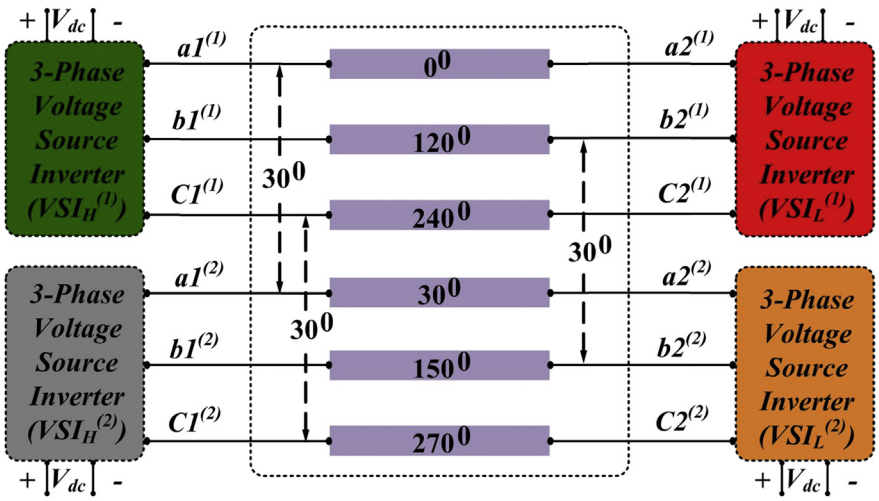

Fig. 2. Configuration of a six-phase asymmetrical (quasi) open-end stator winding motor driven by four customary voltage source inverters (VSIs), one fed on each open-end.

Please cite this article in press as: S. Padmanaban, et al., Power sharing algorithm for vector controlled six-phase AC motor with four customary three-phase voltage source inverter drive, Engineering Science and Technology, an International Journal (2015), http://dx.doi.org/10.1016/j.jestch.2015.02.002

The relationship between six-phase space vectors and two three-phase space vectors is obtained by applying Eqs. (4) and (5) to Eq. (1) and given by:

$$\begin{cases} \bar{x}_1 = \frac{1}{2}\left[\bar{x}^{(1)} + \alpha\bar{x}^{(2)}\right] \\ \bar{x}_5^* = \frac{1}{2}\left[\bar{x}^{(1)} - \alpha\bar{x}^{(2)}\right] \end{cases}, \quad \bar{x}_3 = x_0^{(1)} + jx_0^{(2)}. \tag{6}$$

Inverse transformation of Eq. (6) given by:

$$\begin{cases} \bar{x}^{(1)} = \bar{x}_1 + \bar{x}_5^* \\ x_0^{(1)} = \bar{x}_3 \cdot 1 \end{cases}, \quad \begin{cases} \bar{x}^{(2)} = \alpha^{-1}\left(\bar{x}_1 - \bar{x}_5^*\right) \\ x_0^{(2)} = \bar{x}_3 \cdot j. \end{cases} \tag{7}$$

By Eqs. (6) and (7), it is simplified to represent six-phase (asymmetrical or dual three-phase) open-end stator windings in two three-phase dimensions [5]. It should be considered that:

- The fundamental components with the harmonics of the order $k = 6 \cdot n \pm 1$, ($n = 0, 2, 4\ldots$) are mapped in $\bar{x}_1$ (first sub-space d_1–q_1).
- $k = 6 \cdot n \pm 1$, ($n = 1, 3, 5\ldots$) order harmonics are mapped in $\bar{x}_5^*$ (fifth sub-space d_5–q_5).
- $k = 3 \cdot n$, ($n = 0, 1, 2, 3\ldots$) order harmonics (homopolar components or zero-sequences components) are mapped in the third sub-space $\bar{x}_3$ (third sub-space d_3–q_3).

The multiple space vectors therefore, $\bar{x}_1, \bar{x}_3, \bar{x}_5^*$ are orthogonal to each other in space, i.e. three vectors are independent of each other, hence first sub-space free of odd harmonics and zero-sequence components. Therefore, the complete behavior of the six-phase machine is described by two space vectors $\bar{x}_1$ and $\bar{x}_5^*$ moving arbitrarily in space and controlled independently [10–12].

3. Six-phase open-end induction motor drive

In Fig. 1, the sinusoidally distributed stator windings behavior of the six-phase induction machine is described in stationary reference frame (Eqs. (5) and (6)) by the following space vectors equations:

$$\bar{v}_{S1} = R_S\bar{i}_{S1} + \frac{d\bar{\varphi}_{S1}}{dt}, \quad \bar{\varphi}_{S1} = L_{S1}\bar{i}_{S1} + M_1\bar{i}_{R1}, \tag{8}$$

$$0 = R_R\bar{i}_{R1} - jp\omega_m\bar{\varphi}_{R1} + \frac{d\bar{\varphi}_{R1}}{dt}, \quad \bar{\varphi}_{R1} = M_1\bar{i}_{S1} + L_{R1}\bar{i}_{R1}, \tag{9}$$

$$\bar{v}_{S5} = R_S\bar{i}_{S5} + \frac{d\bar{\varphi}_{S5}}{dt}, \quad \bar{\varphi}_{S5} = L_{S\ell}\bar{i}_{S5}, \tag{10}$$

$$T = 3pM_1\bar{i}_{S1}\cdot j\bar{i}_{R1}, \tag{11}$$

where p represents the pole pair, ω_m the rotor speed and the subscripts S, R represents the stator and rotor reference components. The space vectors currents $\bar{i}_{S1}$ and $\bar{i}_{R1}$ are responsible for the magnetic field in the air gap and $\bar{i}_{S5}$ does not contribute any air gap field and produce only leakage flux [5–8,12].

4. Proposed synchronous reference FOC power sharing algorithm

Fig. 3 depicts the proposed effective power sharing algorithm actually derived from standard synchronous FOC. The total power is shared among the four dc sources by three variables (degree of freedom) in two developed control strategies. In first one, the variables $k_v^{(1)}$, $k_v^{(2)}$ share the voltages between two inverters (VSI_H and VSI_L) of two three-phase open-end stator windings. In second one, the variable k_i share the currents between two three-phase open-end stator windings.

First control strategy deals with voltage sharing, the reference output voltage of first three-phase open-end stator windings ($\bar{v}^{(1)}$) and second three-phase open-end stator windings ($\bar{v}^{(2)}$) are determined by the space vectors $\bar{v}_{S1,ref}$ and $\bar{v}^*$ given by Eq. (6). The reference voltage $\bar{v}^{(1)}$ is produced by the sum of $\bar{v}_H^{(1)}$ and $\bar{v}_L^{(1)}$ reference output voltages by inverters $VSI_H^{(1)}$ and $VSI_L^{(1)}$ for first three-phase open-end windings. Similarly, the reference voltage $\bar{v}^{(2)}$ is produced by the sum of $\bar{v}_H^{(2)}$ and $\bar{v}_L^{(2)}$ reference output voltages by inverters $VSI_H^{(2)}$ and $VSI_L^{(2)}$ for second three-phase open-end windings, then:

$$\bar{v}^{(1)} = \bar{v}_H^{(1)} + \bar{v}_L^{(1)}, \tag{12}$$

$$\bar{v}^{(2)} = \bar{v}_H^{(2)} + \bar{v}_L^{(2)}. \tag{13}$$

By introducing first and second voltage sharing variables say $k_v^{(1)}$ to Eq. (12), $k_v^{(2)}$ to Eq. (13), then output voltage references are predicted as

$$\begin{cases} \bar{v}_H^{(1)} = k_v^{(1)}\bar{v}^{(1)} \\ \bar{v}_L^{(1)} = \left(1 - k_v^{(1)}\right)\bar{v}^{(1)} \end{cases}, \quad \begin{cases} \bar{v}_H^{(2)} = k_v^{(2)}\bar{v}^{(2)} \\ \bar{v}_L^{(2)} = \left(1 - k_v^{(2)}\right)\bar{v}^{(2)}. \end{cases} \tag{14}$$

Eq. (14) allows their maximum dc bus voltage utilization by the inverters, the total power developed by the first and second three-phase open-end stator windings is defined as:

$$P^{(1)} = P_H^{(1)} + P_L^{(1)} = \frac{3}{2}\bar{v}^{(1)}\cdot\bar{i}^{(1)}; \quad P^{(2)} = P_H^{(2)} + P_L^{(2)} = \frac{3}{2}\bar{v}^{(2)}\cdot\bar{i}^{(2)}, \tag{15}$$

where $P_H^{(1)}$, $P_L^{(1)}$ and $P_H^{(2)}$, $P_L^{(2)}$ are the individual powers of inverters $VSI_H^{(1)}$, $VSI_L^{(1)}$ and $VSI_H^{(2)}$, $VSI_L^{(2)}$.

By comparing Eqs. (14) and (15), the individual power generated by each inverters $VSI_H^{(1)}$, $VSI_L^{(1)}$ and $VSI_H^{(2)}$, $VSI_L^{(2)}$ is derived as

$$\begin{cases} P_H^{(1)} = k_v^{(1)}P^{(1)} \\ P_L^{(1)} = \left(1 - k_v^{(1)}\right)P^{(1)} \end{cases}; \quad \begin{cases} P_H^{(2)} = k_v^{(2)}P^{(2)} \\ P_L^{(2)} = \left(1 - k_v^{(2)}\right)P^{(2)}. \end{cases} \tag{16}$$

Therefore, the total power of two three-phase open-end stator windings written in terms of two voltage sharing variables $k_v^{(1)}$ and $k_v^{(2)}$ from Eqs. (15) and (16) can be summarized as [27–29]:

$$\begin{aligned} P &= P^{(1)} + P^{(2)} = \left[P_H^{(1)} + P_L^{(1)}\right] + \left[P_H^{(2)} + P_L^{(2)}\right] = \frac{3}{2}\left[\bar{v}^{(1)}\cdot\bar{i}^{(1)} + \bar{v}^{(2)}\cdot\bar{i}^{(2)}\right] \\ P &= \frac{3}{2}\left[\left(\bar{v}_H^{(1)} + \bar{v}_L^{(1)}\right)\cdot\bar{i}^{(1)} + \left(\bar{v}_H^{(2)} + \bar{v}_L^{(2)}\right)\cdot\bar{i}^{(2)}\right] \\ P &= \frac{3}{2}\left[\left(k_v^{(1)}\bar{v}_H^{(1)} + \left(1 - k_v^{(1)}\right)\bar{v}_L^{(1)}\right)\cdot\bar{i}^{(1)} + \left(k_v^{(2)}\bar{v}_H^{(2)} + \left(1 - k_v^{(2)}\right)\bar{v}_L^{(2)}\right)\cdot\bar{i}^{(2)}\right]. \end{aligned} \tag{17}$$

Both the references ($\bar{v}_H^{(1)}$ and $\bar{v}_L^{(1)}$), ($\bar{v}_H^{(2)}$ and $\bar{v}_L^{(2)}$) should be within the range of obtainable output voltages and they depend solely on their dc bus voltages. The total reference voltages $\bar{v}^{(1)}$ and $\bar{v}^{(2)}$ should satisfy if one inverter voltage saturates, the second inverter should generate the missing quantity of voltage in the corresponding two three-phase open-end stator windings.

Please cite this article in press as: S. Padmanaban, et al., Power sharing algorithm for vector controlled six-phase AC motor with four customary three-phase voltage source inverter drive, Engineering Science and Technology, an International Journal (2015), http://dx.doi.org/10.1016/j.jestch.2015.02.002

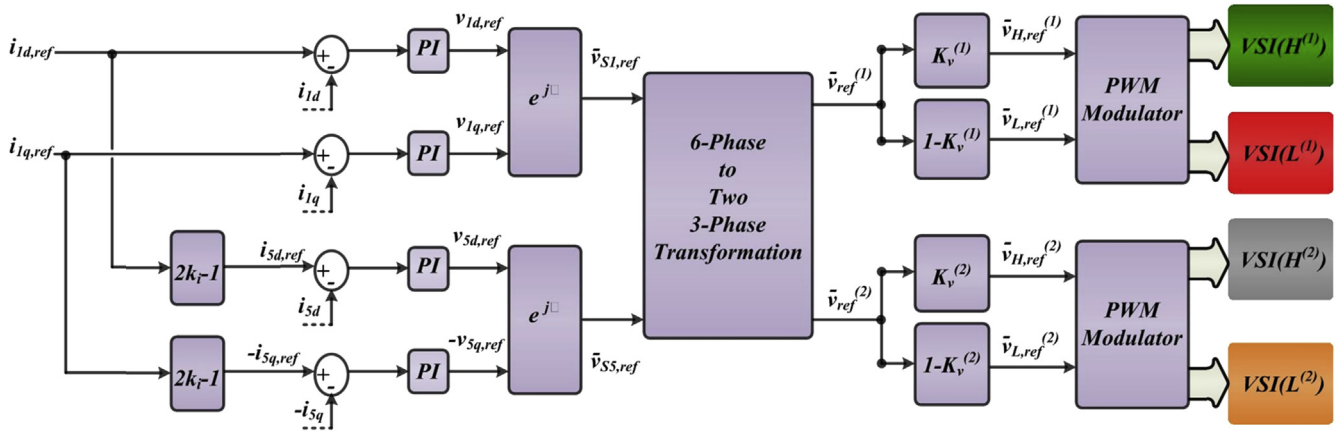

Fig. 3. Complete effective power sharing algorithm with three realizable sharing variables in synchronous field oriented control (FOC).

Second control strategy deals with proper current sharing between two three-phase open-end stator windings. The space vector $\bar{i}_{S1}$ stator current which is determined on the basis of torque and flux commands by Eq. (6) as:

$$\bar{i}_{S1} = \frac{1}{2}\left(\bar{i}^{(1)} + \alpha\bar{i}^{(2)}\right). \tag{18}$$

Introducing the third variable k_i in Eq. (18), leads to:

$$\begin{cases} \frac{1}{2}\bar{i}^{(1)} = k_i\bar{i}_{S1} \\ \frac{1}{2}\alpha\bar{i}^{(2)} = (1-k_i)\bar{i}_{S1}. \end{cases} \tag{19}$$

Now, from the above expression, the first and second three-phase open-end stator windings currents $\bar{i}^{(1)}$ and $\bar{i}^{(2)}$ are obtained as:

$$\begin{cases} \bar{i}^{(1)} = 2k_i\bar{i}_{S1} \\ \bar{i}^{(2)} = 2(1-k_i)\alpha^{-1}\bar{i}_{S1}. \end{cases} \tag{20}$$

By introducing Eq. (20) in Eq. (7), the space vector stator current $\bar{i}_{S5}^{*}$ which produces the leakage fluxes is determined as:

$$\bar{i}_{S5}^{*} = \frac{1}{2}\left(\bar{i}^{(1)} - \alpha\bar{i}^{(2)}\right) = (2k_i - 1)\bar{i}_{S1}. \tag{21}$$

Also, Eq. (21) can be rewritten in equivalent d–q components as

$$\begin{cases} i_{5d} = (2k_i - 1)i_{1d} \\ i_{5q} = -(2k_i - 1)i_{1q}. \end{cases} \tag{22}$$

The total motor power can be determined as [27–29]:

$$P = P^{(1)} + P^{(2)} = 3\bar{v}_{S1}\cdot\bar{i}_{S1} + 3\bar{v}_{S5}\cdot\bar{i}_{S5}. \tag{23}$$

On the basis of Eq. (7), individual space vectors of two three-phase open-end stator winding currents and voltages are calculated as:

$$\begin{cases} \bar{i}^{(1)} = \bar{i}_{S1} + \bar{i}_{S5}^{*} \\ \bar{i}^{(2)} = \alpha^{-1}\left(\bar{i}_{S1} - \bar{i}_{S5}^{*}\right) \end{cases}, \quad \begin{cases} \bar{v}^{(1)} = \bar{v}_{S1} + \bar{v}_{S5}^{*} \\ \bar{v}^{(2)} = \alpha^{-1}\left(\bar{v}_{S1} - \bar{v}_{S5}^{*}\right). \end{cases} \tag{24}$$

By substituting Eq. (24) in Eq. (15) by considering Eq. (21), leads to predict individual power delivered by the two three-phase open-end stator windings as:

$$\begin{aligned} P^{(1)} &= 3k_i\bar{v}_{S1}\cdot\bar{i}_{S1} + 3k_i\bar{v}_{S5}^{*}\cdot\bar{i}_{S1} \\ P^{(2)} &= 3(1-k_i)\bar{v}_{S1}\cdot\bar{i}_{S1} - 3(1-k_i)\bar{v}_{S5}^{*}\cdot\bar{i}_{S1}. \end{aligned} \tag{25}$$

In the characteristic equation of motor given by Eqs. (8) and (10), the space vector $\bar{v}_{S5}^{*}$ (generating the leakage flux in the air-gap only) is negligible in comparison to $\bar{v}_{S1}$ (generating the magnetic flux in the air-gap). Then Eq. (25) can be approximates as:

$$P^{(1)} \cong k_i P; \quad P^{(2)} \cong (1-k_i)P. \tag{26}$$

It has been proved that the third variable k_i introduced in the power equations is good approximation for current sharing between two open-end stator windings.

Finally from Eqs. (16) and (26), the expression for individual power of each inverters and the total power of the motor with three power sharing variables is given by:

$$\begin{aligned} &P_H^{(1)} \cong k_i\cdot k_v^{(1)}P^{(1)}; \quad P_H^{(2)} \cong k_i\cdot k_v^{(2)}P^{(2)} \\ &P_L^{(1)} \cong k_i\cdot\left(1-k_v^{(1)}\right)P^{(1)}; \quad P_L^{(2)} \cong k_i\cdot\left(1-k_v^{(2)}\right)P^{(2)} \\ &P \cong k_i\cdot\left[k_v^{(1)}P_H^{(1)} + \left(1-k_v^{(1)}\right)P_L^{(1)}\right] + (1-k_i) \\ &\qquad\cdot\left[k_v^{(2)}P_H^{(2)} + \left(1-k_v^{(2)}\right)P_L^{(2)}\right]. \end{aligned} \tag{27}$$

Fig. 3 elaborates the complete power sharing algorithm based on synchronous FOC. The d_1–q_1 components of the stator currents which produce the flux and torque in the machine, where d-axis aligned with the rotor flux, displaced by angle ϑ (rotor flux angle). The reference values in synchronous rotating frame of flux $i_{1d,\mathrm{ref}}$ and torque $i_{1q,\mathrm{ref}}$ producing currents are derived from the flux and torque commands. Then, d_1–q_1 components of the reference current are directly determined on the basis of the corresponding d_1–q_1 components current ratio. The stator voltage space vectors whose reference values in stationary reference frames $\bar{v}_{S1,\mathrm{ref}}$ and $\bar{v}_{S5,\mathrm{ref}}$ are determined from P–I (proportional–integral) controller output rotated in rotor flux angle.

Further, standard three-level space vector pulse width modulation (SVPWM) is adopted to regulate each couple of inverter (VSI_H and VSI_L) with two voltage sharing variable to regulate the output voltages as shown in the same Fig. 3 [13,16–19]. It is defined $\bar{v}_{S5,\mathrm{ref}} = 0$, the balanced power sharing by the two three-phase open-end stator windings, i.e. quadrupling the power capability of a single VSI with given voltage and current rating.

Please cite this article in press as: S. Padmanaban, et al., Power sharing algorithm for vector controlled six-phase AC motor with four customary three-phase voltage source inverter drive, Engineering Science and Technology, an International Journal (2015), http://dx.doi.org/10.1016/j.jestch.2015.02.002

5. Verification with simulation tests

To verify the proposed power sharing FOC algorithm, the complete model of ac motor is implemented in numerical simulation software (Matlab/Simulink-PLECS) [30] with the parameters taken from Table 1.

First simulation test deals with balanced condition, obtained by setting the three power sharing variable as $k_v^{(1)} = k_v^{(2)} = \mathbf{1/2}$, $k_i = \mathbf{1/2}$, electro-magnetic torque $T = 53.4$ N m (rated) and rotor speed fixed at $\omega_m = 1440$ rpm (rated). Fig. 4(a) shows the step reference torque command (red color) set to increasing/decreasing between (50−100-−50)% of rated value. It is observed that actual torque (blue color) follows the step variations exactly in every 30 ms.

As expected the synchronous reference frame (first space) currents i_{q1} (blue color) and i_{d1} (violet color), follow the reference torque command and the reference rotor flux command, respectively, as shown by Fig. 4(b) and (c). As determined by Eq. (22) ($k_i = 1/2$), the synchronous reference frame (fifth space) current i_{q5} and i_{d5} (leakage components) are null as shown by Fig. 4(d), which confirms the balanced operation of the ac motor drive.

First (purple color) and second (turquoise color) three-phase open-end stator windings current have a sinusoidal waveform, as shown in Fig. 4(e) and (f); they change according to the torque demand in every 30 ms. It is confirmed that both the two three-phase (six-phase) stator windings currents have the same amplitude in every 30 ms according to torque demand, and the expected 30° phase displacement between them is also noticeable. Hence, the balanced currents operation of ac motor drive in the entire testing period is proved.

Fig. 4(g)–(j) shows the DC link currents of the four inverters (low-pass filtered by time constant $\tau = 2$ ms) $\mathrm{VSI}_{\mathrm{H}}^{(1)}$ (green color), $\mathrm{VSI}_{\mathrm{L}}^{(1)}$ (red color), $\mathrm{VSI}_{\mathrm{H}}^{(2)}$ (gray color), $\mathrm{VSI}_{\mathrm{L}}^{(2)}$ (orange color). DC link currents of four VSIs vary equally in amplitude during every 30 ms, following the behavior given by Eqs. (16), (26) and (27), and ensuring balanced power operation among the VSIs.

The trajectories of stationary reference frame currents are shown in Fig. 5 for an additional verification. Where, Fig. 5(a) confirms the sinusoidal nature of first phase current components i_{sd1} and i_{sq1}, which actually produces the electromagnetic field in the air-gap and its amplitude depends on torque demands. Fig. 5(b) shows that the fifth space current components i_{sd5} and i_{sq5} are null, confirming the balanced operation of the ac motor drive according to Eq. (21) ($k_i = 1/2$). Fig. 5(c) shows that the third space current components i_{sd3} and i_{sq3} are practically zero, confirming that the ac motor drive system is absolutely free of zero-sequence components.

Second simulation test deals with the verification of first control strategy, where the stator voltages are effective shared between each couple of inverters ($\mathrm{VSI_H}$ and $\mathrm{VSI_L}$) of two three-phase open-end stator windings. The three power sharing variables are set to $k_v^{(1)} = \mathbf{1/2–1/3}$, $k_v^{(2)} = \mathbf{1/2–1/3}$, and $k_i = \mathbf{1/2}$, electromagnetic torque is $T = 53.4$ N m (rated) and rotor speed is set to $\omega_m = 1100$ rpm. To avoid inverters saturation (speed directly proportional to voltage), the rotor speed ω_m is reduced from 1440 rpm (rated) to 1100 rpm. From Fig. 6(a) it is observed that actual torque (blue color) exactly follows the set reference torque command (red color). It also clearly indicates that torque is unaffected by the transient introduced in the two power sharing variable ($k_v^{(1)}, k_v^{(2)}$).

Table 1
Parameters taken for simulation software examination of the ac motor.

$P_{\mathrm{rated}} = 8$ kW	$R_S = 0.51\ \Omega$
$I_{\mathrm{S,rated}} = 16\ \mathrm{A_{rms}}$	$R_R = 0.42\ \Omega$
$V_{\mathrm{S,rated}} = 125\ \mathrm{V_{rms}}$	$L_{S1} = 58.2$ mH
$\omega_{\mathrm{S,rated}} = 2\pi 50$ rad/s	$L_R = 58.2$ mH
$P = 2$ (pairs)	$M_1 = 56$ mH
DC bus voltage = 155 V	
Switching frequency = 5 kHz	

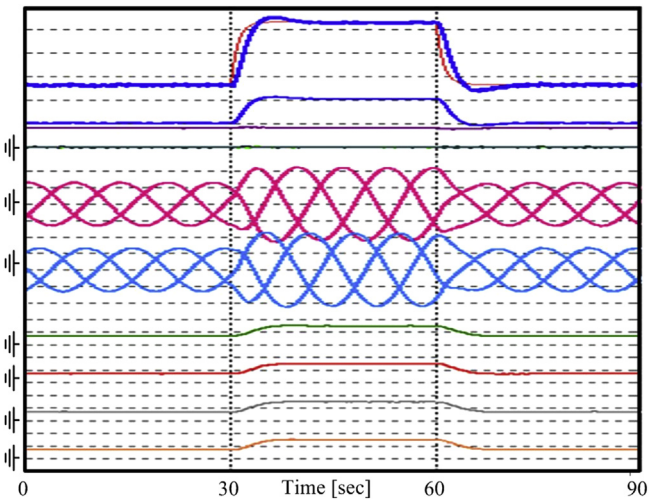

Fig. 4. Behavior of six-phase asymmetrical (quasi) open-end stator windings induction motor in balanced condition. Characteristic waveform in sequential order: a. Torque response with respect to step changes (blue-torque, red-step command). [*Y*-axis scale: 10 N m/div]. b. Torque producing current (first-space) component i_{1q}. [*Y*-axis scale: 10 A/div]. c. Flux producing current (first-space) component i_{1d}. [*Y*-axis scale: 10 A/div]. d. Leakage current (fifth-space) components i_{5q}, i_{5d}. [*Y*-axis scale: 10 A/div]. e. Three-phase current of first open-end stator windings. [*Y*-axis scale: 10 A/div]. f. Three-phase current of second open-end stator windings. [*Y*-axis scale: 10 A/div]. g. DC link current of inverter $\mathrm{VSI}_{\mathrm{H}}^{(1)}$. [*Y*-axis scale: 10 A/div]. h. DC link current of inverter $\mathrm{VSI}_{\mathrm{L}}^{(1)}$. [*Y*-axis scale: 10 A/div]. i. DC link current of inverter $\mathrm{VSI}_{\mathrm{H}}^{(2)}$. [*Y*-axis scale: 10 A/div]. j. DC link current of inverter $\mathrm{VSI}_{\mathrm{L}}^{(2)}$. [*Y*-axis scale: 10 A/div].

As expected, the synchronous reference frame (first space) currents i_{q1} (blue color) and i_{d1} (violet color), follow the reference torque command and the reference rotor flux command, respectively, as shown by Fig. 6(b) and (c). Also in this test, the synchronous reference frame (fifth space) current i_{q5} and i_{d5} (leakage components) are null as shown by Fig. 6(d), as determined by Eq. (22) ($k_i = 1/2$).

First (purple color) and second (turquoise color) three-phase open-end stator windings current (purple color) have a sinusoidal waveform as shown by Fig. 6(e) and (f). Six-phase currents maintain equal amplitude in the whole period confirming balanced current operation according to constant torque; a correct 30° phase displacement between them is observed. It is noted that currents are unaffected by the transient created by the two voltage sharing variables when subjected to a change in their values.

Fig. 6(g)–(j) shows that the DC link currents of four VSIs vary its values according to Eq. (16). Therefore, it is confirmed that sum of power delivered by inverters ($\mathrm{VSI}_{\mathrm{H}}^{(1)}$ and $\mathrm{VSI}_{\mathrm{L}}^{(1)}$) is equal to $P^{(1)}$. In detail, when $k_v^{(1)} = \mathbf{1/2–1/3}$ changes its value at 30 ms, $\mathrm{VSI}_{\mathrm{H}}^{(1)}$ provides only 1/3 of $P^{(1)}$ whereas inverter $\mathrm{VSI}_{\mathrm{L}}^{(1)}$ provides 2/3 of $P^{(1)}$. Their sum correctly maintains the constant power delivered to the first three-phase open-end stator winding. Similarly, the sum of power delivered by inverters ($\mathrm{VSI}_{\mathrm{H}}^{(2)}$ and $\mathrm{VSI}_{\mathrm{L}}^{(2)}$) is equal to $P^{(2)}$. In particular when $k_v^{(2)} = \mathbf{1/2–2/3}$ changes its value at 60 ms, $\mathrm{VSI}_{\mathrm{H}}^{(2)}$ provides only 2/3 of $P^{(2)}$ whereas inverter $\mathrm{VSI}_{\mathrm{L}}^{(2)}$ provides 1/3 of $P^{(2)}$. Their sum correctly maintains the constant power delivered to the second three-phase open-end stator winding. Hence the dc currents of VSIs confirm the effectiveness of first control strategy, sharing the voltages between inverters ($\mathrm{VSI_H}$ and $\mathrm{VSI_L}$) of

Please cite this article in press as: S. Padmanaban, et al., Power sharing algorithm for vector controlled six-phase AC motor with four customary three-phase voltage source inverter drive, Engineering Science and Technology, an International Journal (2015), http://dx.doi.org/10.1016/j.jestch.2015.02.002

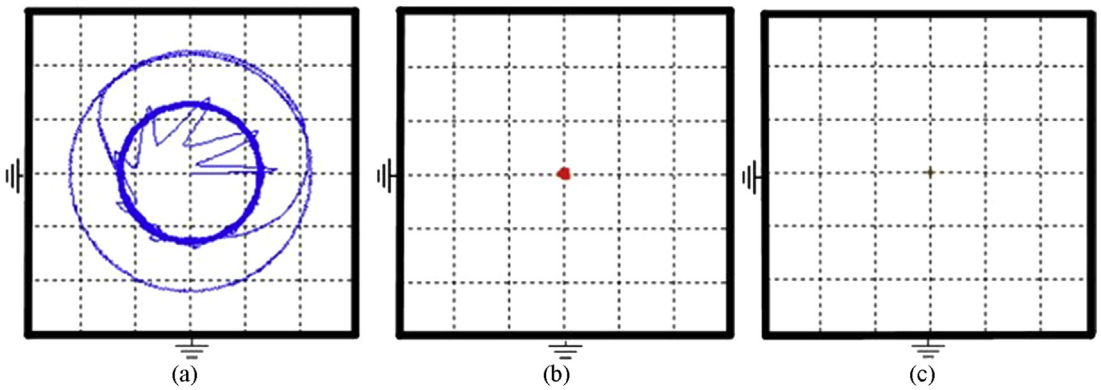

Fig. 5. Response trajectories in stationary reference frame current components. a. i_{s1} vs i_{s1}, b. i_{s5} vs i_{s5}, c. i_{s3} vs i_{s3}. [*X*–*Y*-axis scale: +/−10 A/div].

two three-phase open-end stator windings (according to Eqs. (16) and (27)).

The trajectories of stationary reference frame currents are shown in Fig. 7. Fig. 7(a) shows that the first phase current components i_{sd1} and i_{sq1}, are sinusoidal with steady-state constant amplitude, depending on the given torque demand. This again confirms that both torque and motor currents are unaffected from the transient created by the two voltage sharing variables. Fig. 7(b) shows that the fifth space current components i_{sd5} and i_{sq5} are zero, according to Eq. (21) ($k_i = 1/2$). Fig. 7(c) shows that the third space current components i_{sd3} and i_{sq3} are practically zero, confirming that the ac motor drive system is absolutely free of zero-sequence components.

Third simulation test deals with the verification of second control strategy, where the currents are effectively shared between two three-phase open-end stator windings. The three power sharing variables are set to $k_v^{(1)} = k_v^{(2)} = \mathbf{1/2}$, $k_i = \mathbf{1/2–1/3–2/3}$, electromagnetic torque is $T = 38$ N m, and rotor speed is set to $\omega_m = 1430$ rpm (rated). To avoid over-current delivery from inverters w.r.t. rated power (torque directly proportional to current), the torque reference is reduced from 53.4 N m (rated) to 38 N m. From Fig. 8(a), it is observed that actual torque (blue color) exactly follows the set reference torque command (red color). It also indicates clearly that torque is unaffected by the transient created by current sharing variable k_i when subjected to a change in its value.

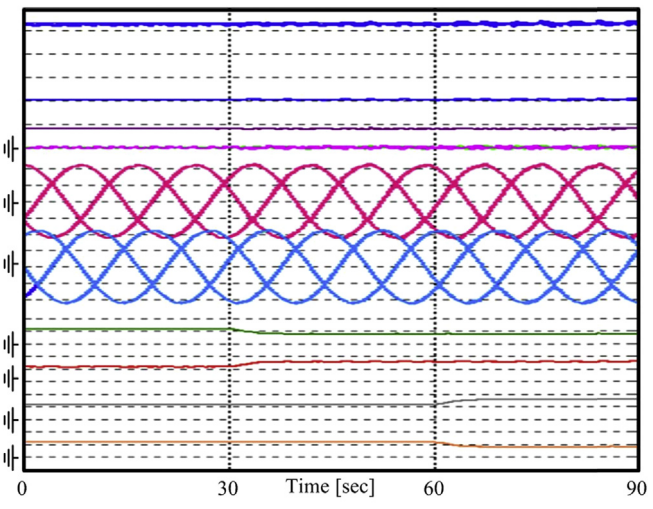

Fig. 6. Behavior of six-phase asymmetrical (quasi) open-end stator windings induction motor in first prediction when unbalanced voltage sharing between each couple of inverters (VSI_H and VSI_L) condition. Characteristic waveform in sequential order: a. Torque response with respect to step changes (blue-torque, red-step command). [*Y*-axis scale: 10 N m/div]. b. Torque producing current (first-space) component i_{1q}. [*Y*-axis scale: 10 A/div]. c. Flux producing current (first-space) component i_{1d}. [*Y*-axis scale: 10 A/div]. d. Leakage current (fifth-space) components i_{5q}, i_{5d}. [*Y*-axis scale: 10 A/div]. e. Three-phase current of first open-end stator windings. [*Y*-axis scale: 10 A/div]. f. Three-phase current of second open-end stator windings. [*Y*-axis scale: 10 A/div]. g. DC link current of inverter $VSI_H^{(1)}$. [*Y*-axis scale: 10 A/div]. h. DC link current of inverter $VSI_L^{(1)}$. [*Y*-axis scale: 10 A/div]. i. DC link current of inverter $VSI_H^{(2)}$. [*Y*-axis scale: 10 A/div]. j. DC link current of inverter $VSI_L^{(2)}$. [*Y*-axis scale: 10 A/div].

As expected the synchronous reference frame (first space) currents i_{q1} (blue color) and i_{d1} (violet color), follows the reference torque command and the reference rotor flux command as shown by Fig. 8(b) and (c). Now, the synchronous reference frame (fifth space) currents i_{q5} and i_{d5} are null up to first 30 ms, proving the balanced operation, as shown in Fig. 8(d). Furthermore, the currents are generated according to Eq. (21) ($k_i = \mathbf{1/2–1/3–2/3}$) at 30 ms and 60 ms, ensuring the proper currents sharing between two three-phase stator windings, as shown in the same Fig. 8(d).

First (purple color) and second (turquoise color) three-phase open-end stator windings current (purple color) have a sinusoidal waveform as shown by Fig. 8(e) and (f). It is observed that until 30 ms both three-phase stator winding currents have the same amplitude, confirming the balanced operation. Then six-phase currents share 1/3 and 2/3 of the total current (power) demand at 30 ms and 60 ms for the reference torque requirement, according to Eq. (20). Furthermore, it is noticed that the correct 30° phase displacement is maintained between the two three-phase stator currents, and the torque is unaffected during the transients of the current sharing variable.

Fig. 8(g)–(j) shows that DC link current of the four VSIs changes its value according to Eq. (26), confirming the current sharing between the two three-phase stator windings. In particular, DC currents have same amplitude until 30 ms; once the current sharing variable changes its value $k_i = 1/2–1/3–2/3$ at 30 ms and 60 ms, it observed that DC currents drops in inverters $VSI_H^{(1)}$ and $VSI_L^{(1)}$ are compensated by increasing DC currents in inverters $VSI_H^{(2)}$ and $VSI_L^{(2)}$, and vice-versa. It is concluded that the total current remains always constant as per torque demand.

The trajectories of stationary reference frame currents are shown in Fig. 9. In particular, Fig. 9(a) shows that the first phase current components i_{sd1} and i_{sq1} have a sinusoidal waveform, with constant amplitude at steady-state, depending on the torque demand. This again confirms that the torque is unaffected by the transient created by the current sharing change. Fig. 9(b) shows the fifth space current components i_{sd5} and i_{sq5}, generated according to Eq. (22) ($k_i = 1/2–1/3–2/3$). This further confirms that the fifth space is responsible for the current sharing between two stator

Please cite this article in press as: S. Padmanaban, et al., Power sharing algorithm for vector controlled six-phase AC motor with four customary three-phase voltage source inverter drive, Engineering Science and Technology, an International Journal (2015), http://dx.doi.org/10.1016/j.jestch.2015.02.002

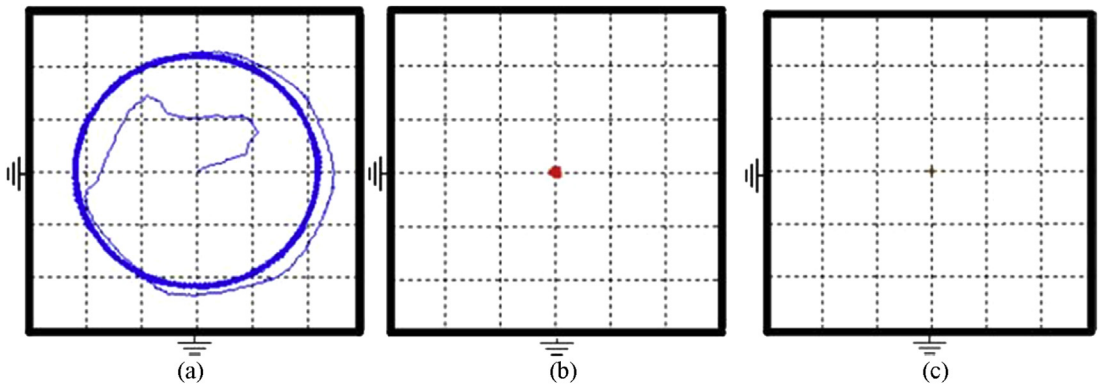

Fig. 7. Response trajectories in stationary reference frame current components. a. i_{s1} vs i_{s1}, b. i_{s5} vs i_{s5}, c. i_{s3} vs i_{s3}. [*X*–*Y*-axis scale: +/−10 A/div].

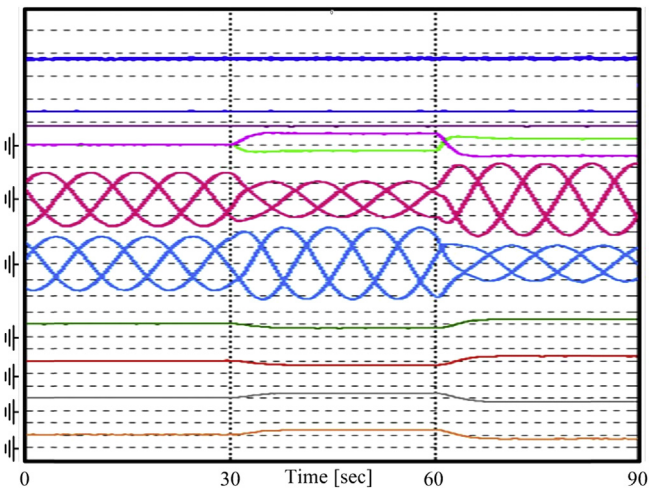

Fig. 8. Behavior of six-phase asymmetrical (quasi) open-end stator windings induction motor in second prediction when unbalanced current sharing between two open-end stator windings. Characteristic waveform in sequential order: a. Torque response with respect to step changes (blue-torque, red-step command). [*Y*-axis scale: 10 N m/div]. b. Torque producing current (first-space) component i_{1q}. [*Y*-axis scale: 10 A/div]. c. Flux producing current (first-space) component i_{1d}. [*Y*-axis scale: 10 A/div]. d. Leakage current (fifth-space) components i_{5q}, i_{5d}. [*Y*-axis scale: 10 A/div]. e. Three-phase current of first open-end stator windings. [*Y*-axis scale: 10 A/div]. f. Three-phase current of second open-end stator windings. [*Y*-axis scale: 10 A/div]. g. DC link current of inverter $VSI_H^{(1)}$. [*Y*-axis scale: 10 A/div]. h. DC link current of inverter $VSI_L^{(1)}$. [*Y*-axis scale: 10 A/div]. i. DC link current of inverter $VSI_H^{(2)}$. [*Y*-axis scale: 10 A/div]. j. DC link current of inverter $VSI_L^{(2)}$. [*Y*-axis scale: 10 A/div].

open-end windings. Fig. 9(c) shows that the third space current components i_{sd3} and i_{sq3} is practically zero, confirming that the ac drive system is absolutely free of zero-sequence components.

Finally, it is confirmed from all this numerical simulation tests that the proposed power sharing algorithm (FOC) is effective, maintaining the constant power delivered to motor irrespective of sharing voltage and/or currents among the two three-phase stator open-end windings.

6. Conclusion

This paper presented an original and effective power sharing algorithm based on field oriented control (FOC) in synchronous reference frame for six-phase (asymmetrical) open-end stator windings motor. Power driver circuit consists of four customary three-phase voltage source inverters (VSIs), each one connected across the open-ends of the stator windings to framed multi-phase inverter drive configuration. The standard three-level space vector modulation is adopted for each VSI to behave as three-level output voltage generator. The proposed power sharing algorithm consists of three variables corresponding to three degrees of freedom in control. Two variables can share the two voltages between two inverters of each two three-phase open-end stator windings. The third variable can share the current between two open-end stator windings. Detailed investigation are carried out by the implementation of the complete ac drive model with power sharing (FOC) algorithm in numerical simulation software, and all the proposed balanced/unbalanced theoretical developments successfully are verified.

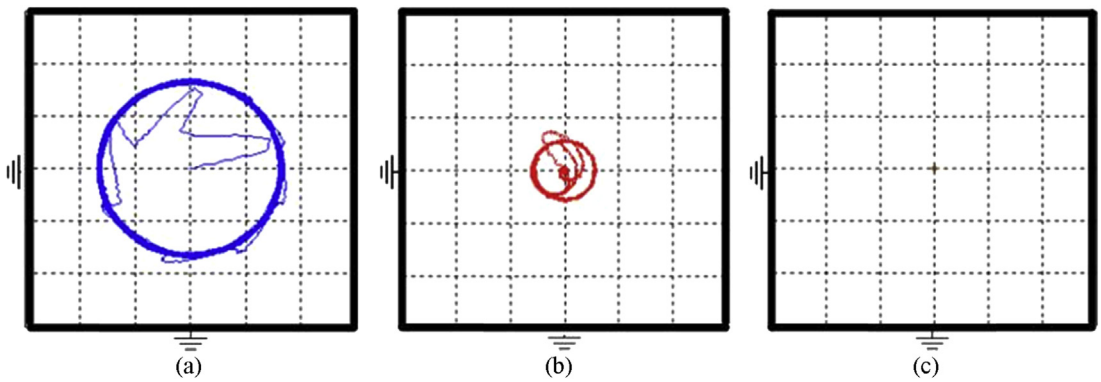

Fig. 9. Response trajectories in stationary reference frame current components. a. i_{s1} vs i_{s1}, b. i_{s5} vs i_{s5}, c. i_{s3} vs i_{s3}. [*X*–*Y*-axis scale: +/−10 A/div].

Please cite this article in press as: S. Padmanaban, et al., Power sharing algorithm for vector controlled six-phase AC motor with four customary three-phase voltage source inverter drive, Engineering Science and Technology, an International Journal (2015), http://dx.doi.org/10.1016/j.jestch.2015.02.002

Acknowledgement

We authors would like to acknowledge Ministry of University Research (**MIUR**), Government of Italy, for providing research fund for carry out this research activity with Power Electronics Laboratory, Department of Electrical, Electronics and Information Engineering, University of Bologna, Viale Risorgimento 2, Bologna-40136, Italy.

References

[1] E. Levi, Multiphase electric machines for variable-speed applications, IEEE Trans. Ind. Electron. 55 (5) (2008) 1893–1909.
[2] E. Levi, R. Bojoi, F. Profumo, H.A. Toliyat, S. Williamson, Multiphase induction motor drives – a technology status review, IET Electr. Power Appl. J. 1 (4) (2007) 489–516.
[3] W. Cao, B.C. Mecrow, G.J. Atkinson, J.W. Bennett, D.J. Atkinson, Overview of electric motor technologies used for more electric aircraft (MEA), IEEE Trans. Ind. Electron. 59 (9) (2012) 3523–3531.
[4] M. Jones, E. Levi, Series connected quasi-six-phase two-motor drives with independent control, J. Math. Comput. Simul. 71 (2006) 41–424. Elsevier Publications.
[5] Y. Zhao, T.A. Lipo, Space vector PWM control of dual three-phase induction machine using vector space decomposition, IEEE Trans. Ind. Appl. 31 (5) (1995) 1100–1109.
[6] R. Bojoi, F. Farina, F. Profumo, A. Tenconi, Dual three-phase induction machine drives control—a survey, IEE J. Trans. Ind. Appl. 126 (4) (2006).
[7] R. Bojoi, M. Lazzari, F. Profumo, A. Tenconi, Digital field oriented control of dual three-phase induction motor drives, IEEE Trans. Ind. Appl. 39 (2003) 75–760.
[8] R. Bojoi, F. Farina, G. Griva, F. Profumo, A. Tenconi, Direct torque control for dual three-phase induction drives, IEEE Trans. Ind. Appl. 41 (6) (2005) 1627–1636.
[9] G.K. Singh, K. Nam, S.K. Lim, A simple indirect field-oriented control scheme for multiphase induction machine, IEEE Trans. Ind. Electron. 52 (4) (2005) 1177–1184.
[10] A. Tessarolo, C. Bassi, Stator harmonic currents in VSI-fed synchronous motors with multiple three-phase armature windings, IEEE Trans. Energy Convers. 25 (4) (2010) 974–982.
[11] R.H. Nelson, P.C. Krause, Induction machine analysis for arbitrary displacement between multiple winding sets, IEEE Trans. Power Apparatus Syst. (1974) 841–848.
[12] G. Grandi, A. Tani, G. Serra, Space vector modulation of six-phase VSI based on three-phase decomposition, in: Proceeding IEEE 19th International Conference Symposium on Power Electronics, Electrical Drives, SPEEDAM'08, Taormina, Italy, 2008, pp. 674–679.
[13] G. Grandi, C. Rossi, A. Lega, D. Casadei, Multilevel operation and input power balancing for a dual two-level inverter with insulated dc sources, IEEE Trans. Ind. Appl. 44 (6) (2008) 1815–1824.
[14] N. Bodo, E. Levi, M. Jones, Investigation of carrier-based PWM techniques for a five-phase open-end winding drive topology, IEEE Trans. Ind. Electron. 60 (5) (2013) 2054–2065.
[15] J. Prieto, M. Jones, F. Barrero, E. Levi, S. Toral, Comparative analysis of discontinuous and continuous PWM techniques in VSI-fed five-phase induction motor, IEEE Trans. Ind. Electron. 58 (12) (2011) 5324–5335.
[16] O. Dordevic, E. Levi, M. Jones, A vector space decomposition based space vector PWM algorithm for a three-level seven-phase voltage source inverter, IEEE Trans. Power Electron. 28 (2) (2013) 637–649.
[17] M. Jones, N. Satiawan, N. Bodo, E. Levi, A dual five-phase space vector modulation algorithm based on the decomposition method, IEEE Trans. Ind. Appl. 48 (6) (2012) 2110–2120.
[18] K. Marouani, L. Baghli, D. Hadiouche, A. Kheloui, A. Rezzoug, A new PWM strategy based on a 24-sector vector space decomposition for a six-phase VSI-fed dual stator induction motor, IEEE Trans. Ind. Electron. 55 (5) (2008) 1910–1920.
[19] O. Lopez, D. Dujic, M. Jones, F. Freijedo, J. Doval-Gandoy, E. Levi, Multidimensional two-level multiphase space vector PWM algorithm and its comparison with multi frequency space vector PWM method, IEEE Trans. Ind. Electron. 58 (2) (2011) 465–475.
[20] L. Alberti, N. Bianchi, Experimental tests of dual three-phase induction motor under faulty operating condition, IEEE Trans. Ind. Electron. 59 (5) (2012) 2041–2048.
[21] F. Meinguet, P. Sandulescu, X. Kestelyn, E. Semail, A method for fault detection and isolation based on the processing of multiple diagnostic indices: application to inverter faults in AC drives, IEEE Trans. Vehic. Technol. 62 (3) (2013) 995–1009.
[22] J.M. Apsley, De-rating of multiphase induction machines due to supply imbalance, IEEE Trans. Ind. Appl. 46 (2) (2010) 798–805.
[23] I.P. Georgakopoulos, E.D. Mitronikas, A.N. Safacas, Detection of induction motor faults in inverter drives using inverter input current analysis, IEEE Trans. Ind. Electron. 58 (9) (2011) 4365–4373.
[24] F. Betin, G. Capolino, Shaft positioning for six-phase induction machines with open phases using variable structure control, IEEE Trans. Ind. Electron. 59 (6) (2012) 2612–2620.
[25] G. Grandi, A. Tani, P. Sanjeevikumar, D. Ostojic, Multi-phase multi-level ac motor drive based on four three-phase two-level inverters, in: Proceeding IEEE 20th International Conference Symposium on Power Electronics, Electrical Drives, SPEEDAM'10, Pisa, Italy, 2010, pp. 1768–1775.
[26] G. Grandi, P. Sanjeevikumar, Y. Gritli, F. Filippetti, Experimental investigation of fault-tolerant control strategies for quad-inverter converters, in: Proceeding IEEE International Conference on Electrical System for Aircraft, Railway and Ship Propulsion, ESARS'12, Bologna, Italy, 2012.
[27] A. Tani, M. Mengoni, L. Zarri, G. Serra, D. Casadei, Control of multi-phase induction motors with an odd number of phases under open circuit faults, IEEE Trans. Power Electron. 27 (2) (2012) 565–577.
[28] G. Grandi, G. Serra, A. Tani, General analysis of multiphase systems based on space vector approach, in: Proceeding International Power Electronics and Motion Control Conference, EPE-PEMC'06, Portoroz, Slovenia, 2006, pp. 834–840.
[29] A. Tessarolo, G. Zocco, C. Tonello, Design and testing of a 45-MW100-Hz quadruple-star synchronous motor for a liquefied natural gas turbo-compressor drive, IEEE Trans. Ind. Appl. 47 (3) (2011) 1210–1219.
[30] H. Abu-Rub, A. Iqbal, J. Guzinski, High Performance Control of AC Drives with Matlab/Simulink Models, first ed., John Wiley & Sons Ltd., Publications, UK, 2012.

Please cite this article in press as: S. Padmanaban, et al., Power sharing algorithm for vector controlled six-phase AC motor with four customary three-phase voltage source inverter drive, Engineering Science and Technology, an International Journal (2015), http://dx.doi.org/10.1016/j.jestch.2015.02.002